

FIXED FIELD ALTERNATING GRADIENT ACCELERATORS (FFAG) FOR HADRON CANCER THERAPY

E. Keil*, CERN, CH1211 Geneva 23, Switzerland; D. Trbojevic†, BNL, Upton, Long Island, NY 11973-5000, USA; A.M. Sessler‡, LBNL, Berkeley, CA 94720, USA

Abstract

Cancer accelerator therapy continues to be ever more prevalent with new facilities being constructed at a rapid rate. Some of these facilities are synchrotrons, but many are cyclotrons and, of these, a number are FFAG cyclotrons. The therapy method of spot scanning requires many pulses per second (typically 200 Hz), which can be accomplished with a cyclotron (in contrast with a synchrotron). We briefly review commercial scaling FFAG machines and then discuss recent work on non-scaling FFAGs, which may offer the possibility of reduced physical aperture and a large dynamic aperture. However, a variation of tune with energy implies the crossing of resonances during the acceleration process. A design can be developed such as to avoid intrinsic resonances, although imperfection resonances must still be crossed. Parameters of two machines are presented; a 250 MeV proton therapy accelerator and a 400 MeV carbon therapy machine.

INTRODUCTION

A very interesting study of a series of scaling radial-sector FFAGs (three machines) for carbon cancer therapy has been undertaken by Misu et al.[1], who describe many advantages of an FFAG, but point out major difficulties: (i) The radius of the top FFAG is rather large (11 m). (ii) The aperture of magnets is rather large (65 cm). (iii) The dynamic aperture in the low energy FFAG is rather small (80% of the beam is lost during acceleration). (iv) The rf frequency is forced to be rather low (in the MHz range so as to cover the aperture).

In this contribution we build upon the work of Misu et al. by considering the use of non-scaling radial-sector FFAGs for therapy. We show that we can overcome their difficulties by using non-scaling FFAGs. We propose the same ECR ion source, but then follow it immediately with an RFQ that accelerates the ions to a few MeV/u. Then we invoke a first FFAG ring to accelerate by a factor of three in momentum from the output of the RFQ to the injection energy of the second FFAG ring, 31 MeV/u for protons and 65 MeV/u for C⁶⁺ ions. The latter also accelerate by a factor of three in momentum. Thus the final kinetic energies are 250 MeV for protons and 400 MeV/u for C⁶⁺ ions. By the use of superconducting magnets we address difficulty

no. 1. The non-scaling (in contrast with a scaling) FFAG addresses difficulty no. 2. A non-scaling FFAG is almost linear and hence has a large dynamic aperture, so difficulty no. 3 is addressed. Finally, because the aperture is reduced, compared with the Misu et al design, higher frequency RF may be employed, and thus item no. 4 is also addressed.

The down-side of a non-scaling FFAG is that the tune varies during acceleration and, therefore, transverse resonances must be crossed. We explore this subject and determine the necessary rate of acceleration so as not to unacceptably disturb the ion beam. We design the machine so as not to cross the intrinsic half-integral resonance (although the 1/3 and higher order resonances are crossed), but imperfection resonances are crossed. This puts a restriction on a combination of the magnet imperfections and the rate of acceleration.

Table 1: Factors β and γ , momentum p , magnetic rigidity $B\rho$ in the 3.5 to 250 MeV kinetic energy E proton rings

	Inj 1	Ref 1	Transf	Ref 2	Ext 2
β	0.086	0.170	0.251	0.460	0.613
γ	1.004	1.015	1.033	1.126	1.266
E/MeV	3.49	13.8	30.97	118	250
$p/\text{MeV}/c$	81.0	162	243	486	729
$B\rho/\text{Tm}$	0.27	0.54	0.81	1.62	2.43

FFAG LATTICES

The parameters in Tabs. 1 and 2 are those of two sets of FFAG rings. The first set accelerates protons from 20 to 77 MeV, and from 77 to 250 MeV kinetic energy, respectively[2]. The second set is derived from [3], and accelerates C⁶⁺ ions from 9 to 65, and from 65 to 400 MeV/u kinetic energy. The reference momentum is at the average momentum between injection and extraction. The ratio of the momenta at extraction and injection is about three. Hence, acceleration happens between relative momentum errors $\Delta p/p \approx -0.5$ at injection and $\Delta p/p \approx +0.5$ at extraction. The number of periods is 35 in all four machines. The lengths of the elements and the periods, and the circumference of Ring 2 are 3/2 of those in Ring 1, allowing the installation of Ring 2 around Ring 1.

The relativistic factors β and γ , the energies and momenta in the four rings are listed in Tabs. 1 and 2. In all rings, the momenta and the magnetic rigidities between injection, reference and extraction are in the ratio 1:2:3 by design. The magnetic rigidities in the C⁶⁺ rings are a fac-

* Eberhard.Keil@t-online.de

† trbojevic@bnl.gov, supported by US Department of Energy contract DE-AC02-98CH10886

‡ AMSessler@lbl.gov, supported by the U.S. Department of Energy under Contract No. DE-AC03-76SF00098

tor 2.63 higher than in the corresponding proton rings. This factor is equal to the ratio of the momenta divided by the ratio of the charges.

Table 2: Factors β and γ , momentum p and magnetic rigidity $B\rho$ in the C^{6+} rings from 9 to 400 MeV/u kinetic energy per nucleon E/u

	Inj 1	Ref 1	Transf	Ref 2	Ext 2
β	0.139	0.251	0.355	0.577	0.713
γ	1.010	1.033	1.069	1.225	1.426
$p/\text{GeV}/c$	1.57	2.91	4.24	7.89	11.5
$E/u/\text{MeV}$	9.13	31.0	64.9	209	400
$B\rho/\text{Tm}$	0.87	1.62	2.36	4.38	6.37

Table 3 shows the cell parameters of the proton ring from 31 to 250 MeV kinetic energy, and of the C^{6+} ring from 65 to 400 MeV/u kinetic energy. Lengths, bending angles, fields and gradients are taken on the reference orbit. By design, the ratio of the reference momenta in the two rings for protons and the two rings for C^{6+} ions is three. The magnetic fields in the higher energy rings are twice those in the lower energy rings; the gradients in the higher energy rings are 4/3 of those in the lower energy rings.

Table 3: Cell and magnet parameters of the proton rings from 31 to 250 MeV kinetic energy and of the C^{6+} ring from 65 to 400 MeV/u kinetic energy for focusing magnets F and defocusing magnets D

Parameter	Protons	C^{6+}
Cell length (mm)	814	857
F length (mm)	90	110
F angle (mrad)	-16.7	-8.8
F field (T)	-0.300	-0.350
F gradient (T/m)	41.2	87.9
D length (mm)	220	220
D angle (mrad)	213.0	197.1
D field (T)	1.56	3.928
D gradient (T/m)	-28.9	-76.5
Short straight (mm)	66.7	65.2
Long straight (mm)	280.8	280.7

The magnets in the C^{6+} rings are assumed to be superconducting magnets. The magnets in the proton rings may be either room-temperature or permanent magnets, looking more like quadrupoles than conventional combined function magnets, since their characteristic length X , i.e. the negative ratio of field and gradient, is of the order of the aperture radius or smaller. X is the lateral distance between the reference orbit and the zero of the magnetic field; $X > 0$ implies that the magnetic field vanishes in the direction away from the ring centre. In the F magnets with $X_F = 7.3$ mm the field vanishes well inside the aperture. In the D magnets with $X_D = -54$ mm the field vanishes close to the edge of the aperture, which could be half

quadrupoles. Knowing the extreme lateral displacements of the beam within the entire acceleration range, and allowing for betatron oscillations and orbit offsets yields the horizontal aperture.

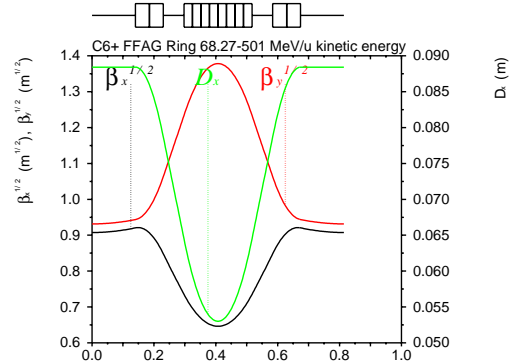


Figure 1: Optical functions $\sqrt{\beta_x}$, $\sqrt{\beta_y}$, and dispersion D_x in a cell of the C^{6+} ring from 69 to 501 MeV/u kinetic energy at the reference momentum

Fig. 1 shows the optical functions $\sqrt{\beta_x}$, $\sqrt{\beta_y}$, and dispersion D_x in a cell of the C^{6+} ring from 69 to 501 MeV/u kinetic energy at the reference momentum. Tab. 4 gives the beam parameters from PTC[4].

Table 4: Beam Parameters phase advance/cell μ , β -functions and dispersion D for the proton ring from 31 to 250 MeV kinetic energy and for the C^{6+} ring from 65 to 400 MeV/u kinetic energy from PTC

Parameter	Protons	C^{6+}
Max H orbit swing (m)	0.094	0.098
H μ at inj	0.381	0.386
V μ at inj	0.410	0.435
H μ at ext	0.113	0.130
V μ at ext	0.082	0.082
Max H β at inj (m)	1.768	1.961
Max H β at ext (m)	0.946	0.855

Fig. 2 shows the variation of the phase advances in a cell of the C^{6+} ring with the relative momentum error $\Delta p/p$. The phase advances at $\Delta p/p = 0$ are design parameters, those for $\Delta p/p \neq 0$ are the result of a calculation with PTC. The tunes vary between from about 13.5 to about 4.5 horizontally, and from about 15.2 to 2.9 vertically. Hence, 9 integral and 21 half-integral resonances are crossed horizontally, and 13 integral and 25 half-integral resonances vertically. Even more resonances of higher order are crossed.

Fig. 3 shows the horizontal β -function along a cell for $-0.5 \leq \Delta p/p \leq 0.5$ in steps of 0.1. The largest and smallest value of β_x occur at $\Delta p/p = -0.5$, due to the proximity of the half-integral stop band. This indicates the price to be paid for the large range of acceleration by a factor of three

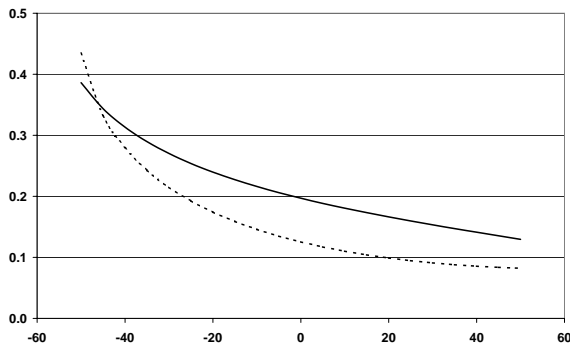


Figure 2: Variation of the phase advances, $\mu_x/2\pi$ horizontally (full line) and $\mu_y/2\pi$ vertically (dashed line), in a cell of the 400 MeV/u C^{6+} ring with the relative momentum error $\Delta p/p$ in percent

in momentum. Fig. 4 shows the horizontal orbit along a cell for $-0.5 \leq \Delta p/p \leq 0.5$ in steps of 0.05.

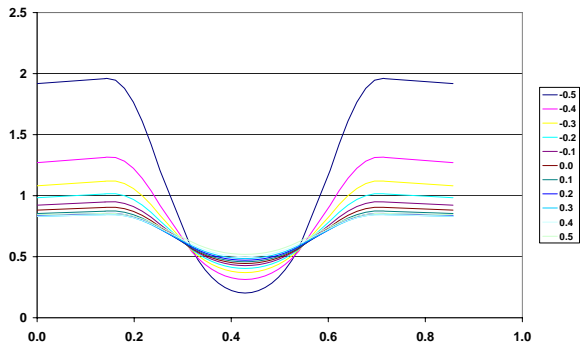


Figure 3: Horizontal β -function along a cell of the 400 MeV/u C^{6+} ring for momentum errors in the the range $-0.5 \leq \Delta p/p \leq +0.5$ in steps of 0.1

RF SYSTEMS

In the proton ring between 31 and 250 MeV kinetic energy, the revolution frequency varies between 2.64 and 6.45 MHz from the variation of the proton speed, neglecting the small contribution of the path length change. If the proton ring between 3.5 and 31 MeV has $2/3$ of the circumference of the larger proton ring, the revolution frequency varies between 1.36 and 3.96 MHz. In order to achieve a transfer of the bunches into buckets, the ratio of harmonic numbers in the high and low energy ring must be a multiple of $3/2$, and the minimum values are $h=3$ and $h=2$, respectively. Hence, the RF frequencies must be varied between multiples of 2.7 and 7.9 MHz in the low energy proton ring, and between the same multiples of 7.9 and 19.4 MHz in the high energy proton ring. The transfer between the two proton rings happens at an RF frequency that is a multiple of 7.9 MHz. The figures for the C^{6+} rings are similar, be-

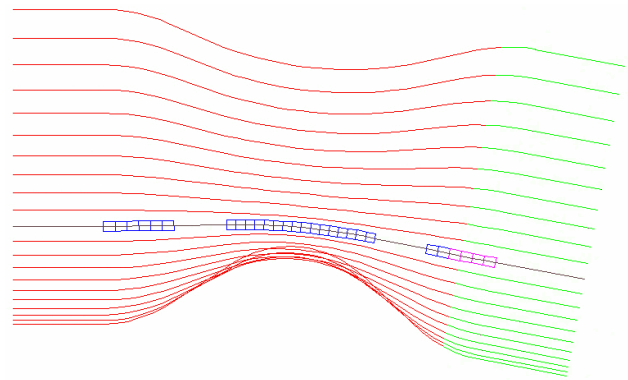


Figure 4: Horizontal orbits along a cell of the 250 MeV proton ring for momentum errors in the the range $-0.5 \leq \Delta p/p \leq 0.5$ in steps of 0.05

tween 3.5 and 10.1 MHz, and between 10.1 and 22.5 MHz with the transfer at 10.1 MHz. A circumference ratio closer to unity than $3/2$, e.g. $4/3$ or $5/4$, increases the minimum harmonic numbers and the minimum RF frequencies.

CONCLUSIONS

In this paper we have presented two complexes of accelerators suitable for cancer therapy. Both involve non-scaling FFAGs. The first complex involves an ion source for protons, an RFQ, and then two FFAG rings bringing the protons to 250 MeV, with a final ring circumference of only 28.5 m. The second complex involves a carbon ion source, an RFQ, and two FFAG rings, finally bringing the carbon ions to 400 MeV per nucleon, with a final ring circumference of only 30 m. The transfers happen at 31 MeV for protons and at 65 MeV/u for carbon.

The FFAG cyclotrons, like all cyclotrons, but different from synchrotrons, allow for the advantageous therapy mode of spot scanning. Compared to scaling FFAGs, namely spiral sector cyclotrons, the non-scaling devices described here have small circumference (thus are compact), small aperture magnets (thus saving on magnet complexity and cost and, most importantly, allowing the use of high frequency RF), and are linear machines (so the dynamic aperture is large). The complexity is the crossing of imperfection resonances, but we show that with reasonably fast acceleration that is no problem.

Detailed engineering, followed by cost estimates, is still to be done. However, our work indicates that further study of non-scaling FFAGs for cancer therapy is appropriate.

REFERENCES

- [1] T. Misu et al., Phys. Rev. STAB **7** (2004) 094701.
- [2] D. Trbojevic et al., subm. to Proc. Cyclotron 2004 (2004).
- [3] E. Keil et al., subm. to Proc. FFAG04 Workshop (2004).
- [4] F. Schmidt et al., KEK-REPORT-2002-3 (2002)